LANGMUIR Article
Cite This: Langmuir 2020, 36, 311−317 pubs.acs.org/Langmuir

Unusual Effect of Iodine Ions on the Self-Assembly of Poly(ethylene glycol)-Capped Gold Nanoparticles

Wenjie Wang,*[,†] Hyeong Jin Kim,[‡] Wei Bu,[∥] Surya Mallapragada,[‡] and David Vaknin*[,§]

[†]Division of Materials Sciences and Engineering, Ames Laboratory, U.S. DOE, Ames, Iowa 50011, United States
[‡]Ames Laboratory, and Department of Chemical and Biological Engineering and [§]Ames Laboratory, and Department of Physics and Astronomy, Iowa State University, Ames, Iowa 50011, United States
[∥]NSF's ChemMatCARS, University of Chicago, Chicago, Illinois 60637, United States

Supporting Information

ABSTRACT: We use synchrotron X-ray reflectivity and grazing incidence small-angle X-ray scattering to investigate the surface assembly of the poly(ethylene glycol) (PEG)-grafted gold nanoparticles (PEG-AuNPs) induced by different salts. We find that NaCl and CsCl behave as many other electrolytes, namely, drive the PEG-AuNPs to the vapor/suspension interface to form a layer of single-particle depth and organize them into very high-quality two-dimensional (2D) hexagonal crystals. By contrast, NaI induces the migration of PEG-AuNPs to the aqueous surface at much higher surface densities than the other salts (at similar concentrations). The resulting 2D ordering at moderate NaI concentrations is very short ranged, and at a higher NaI concentration, the high-density monolayer is amorphous. Considering NaCl, CsCl and the majority of salts behave similarly, this implicates the anomaly of iodine ion (I^-) in this unusual surface population. We argue that the influence of most electrolytes on the PEG corona preserves the polymer in the θ-point with sufficient flexibility to settle into a highly ordered state, whereas I^- has a much more severe effect on the corona by collapsing it. The collapsed PEG renders the grafted AuNP a nonspherical shaped complex that, although packs at high density, cannot organize into a 2D ordered arrangement.

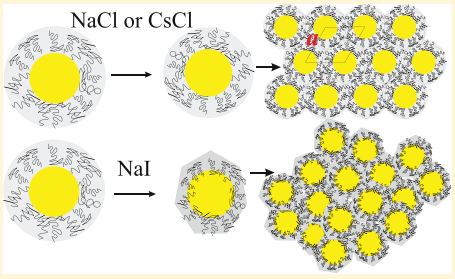

INTRODUCTION

Salts in solutions promote aqueous surface self-assembly of nanoparticles (NPs) that are grafted with nonionic water-soluble polymers. Recently, it has been demonstrated that gold nanoparticles (AuNPs) grafted with poly(ethylene glycol) (PEG) form homogeneous aqueous suspensions, and they self-assemble into highly ordered two- and three-dimensional superstructures under various modifications of the suspension.[1−3] Adding electrolytes or poly-electrolytes to the suspension drives PEG-AuNPs to the vapor−liquid interface to form a monoparticle layer, reminiscent of a Gibbs monolayer.[1,4,5] Furthermore, beyond a threshold salt concentration (salt-specific), the surface-bound PEG-AuNPs crystallize into two-dimensional (2D) hexagonal superlattices with a lattice constant that can be controlled by a specific salt and its concentration.[4,5] At sufficiently high salt concentrations, small-angle X-ray scattering studies reveal that PEG-AuNPs assemble into three-dimensional (3D) superlattices in the bulk suspension or precipitate.[2] In fact, the assembly of PEG-AuNPs into 2D superlattices is so robust that it can be induced at high or low pH values and also with a plethora of salts.[4,5] Based on the experimental results of various electrolyte species, it is believed that the grafted PEG is in the θ-point state[1] and that the effectiveness of ions in driving self-assembly follows to a good approximation the Jones−Dole ionic-coefficient series.[4]

The grafted PEG on the surface of the AuNPs, as other surface ligands, mediates the interparticle interactions that determine the spatial arrangement of AuNPs, such as ordered or disordered arrangement, and interparticle spacing.[6−10] Ascertaining the conformational state (i.e., coiled or collapsed) of PEG and correlating it to the medium conditions (i.e., salt species and concentrations) and the spatial arrangements of PEG-AuNPs at the aqueous surfaces are still an open question. Here, we explore two monovalent salts, CsCl and NaI, that lead to the surface assembly of PEG-AuNPs and use previous results with NaCl,[1] which allows us to shed more light on the effect of cations (i.e., Na^+ and Cs^+) and anions (i.e., Cl^- and I^-) on the grafted PEG. To determine the structure of the assembled PEG-AuNPs in the presence of these salts, we use synchrotron X-ray scatteringfrom liquid surfaces,[11] methods that have been applied to various systems.[12−16] Based on the synchrotron data, the surface number density of the surface-bound PEG-AuNPs and their 2D arrangement can be obtained. We also employ the dynamic light scattering (DLS) technique to determine the hydrodynamic radius of the PEG-AuNPs in salty aqueous suspensions, which enables us to determine the state of PEG corona (e.g., coil or globule[17]).

Received: September 23, 2019
Revised: December 11, 2019
Published: December 16, 2019

DOI: 10.1021/acs.langmuir.9b02966
Langmuir 2020, 36, 311−317

EXPERIMENTAL DETAILS

Materials. Citrate-stabilized AuNPs of average nominal 10 nm diameter were purchased from Ted Pella, Inc, and these were grafted with poly(ethylene glycol) methyl ether thiol (PEG-SH, average molecular weight 6000 Da; Sigma-Aldrich) through thiol-gold chemistry. The PEG-capped AuNPs (PEG-AuNPs) were prepared by using a straightforward ligand exchange and centrifugation method as documented previously.[1]

X-ray Measurements Setup. X-ray reflectivity (XRR) and grazing incidence small-angle scattering (GISAXS) were conducted at beamline 15-ID-C, NSF's ChemMatCARS of the Advanced Phone Source (APS) at Argonne National Laboratory on a liquid surface reflectometer. A monochromatic X-ray beam of energy 10 keV (wavelength λ = 1.2398 Å) is deflected onto the liquid surface (designated as the *xy*-plane) with the desired angle of incidence, α_i, by a Ge(111) steering crystal. An ionization chamber is placed right before the sample to monitor the incident beam intensity. A Pilatus 100K detector with the pixel size 0.172 × 0.172 mm^2 is mounted about 1074 mm away from the sample center to collect XRR and GISAXS signals. The measured XRR data are described as a function of Q_z ($Q_z = 4\pi \sin \alpha_i/\lambda$), which is the vertical component of the scattering vector **Q**. The GISAXS intensity patterns as a function of **Q** are described in terms of the horizontal component Q_{xy} ($\approx 4\pi \sin(\Phi/2)/\lambda$, Φ being the horizontal in-plane scattering angle) and the vertical component Q_z ($= 2\pi(\sin \alpha_i + \sin \alpha_f)/\lambda$, α_f being the exit angle with respect to the surface). GISAXS data were collected below the critical angle for total reflection, α_c, to exploit surface sensitivity. The measured XRR, $R(Q_z)$, is presented here after normalization to the calculated Fresnel reflectivity of an ideally flat surface R_F of the solutions. For synchrotron X-ray characterization, high concentrations of stock solutions for NaI and CsCl were each prepared at 5 M (MilliQ water at 18.2 MΩ cm). A suspension of PEG-AuNPs contained in a shallow trough for X-ray measurements started with a volume of ∼1.5 mL, and the salt concentration was adjusted stepwise by adding ∼150 μL of stock solution to obtain 0.5, 1.0, and 1.5 M of salt concentration. The trough containing the sample was encapsulated in a helium-purged chamber during X-ray measurements to lower potential beam radiation damage and the background scattering. Direct surface tension (ST) measurements with a commercial tensiometer, using a filter paper Wilhelmy plate or a Pt ring as probes, in principle, can also provide aqueous surface activity information on Gibbs monolayers. However, we have found that the various ST probes are prone to contamination by PEG, yielding irreproducible ST results. We therefore decided not to pursue these measurements as they are not relevant to the main message of this study.

Dynamic Light Scattering. Dynamic light scattering (DLS) measurements were conducted (using a Nano ZS90 ZEN3690, Malvern, U.K.) to determine the hydrodynamic diameter (D_h) distribution of bare AuNP and PEG-capped AuNPs in aqueous suspensions in the presence and absence of salts, i.e., NaCl, NaI, and CsCl. All of the tested solutions were assumed to have the viscosity of water when extracting the hydrodynamic size distributions. To estimate the effect of viscosity on D_h, the viscosities of salt solutions at various concentrations were calculated with the empirical equation of Jones−Dole.[18,19] Applying these estimated viscosity values to the DLS spectral analysis lowers D_h distribution by a marginal ∼5% on average.

RESULTS AND DISCUSSION

X-ray Reflectivity. Figures 1a and 2a show normalized reflectivities, R/R_F, from aqueous surfaces of PEG-AuNPs suspensions with varying concentrations of CsCl and NaI, respectively, as indicated. The solid lines superimposed on the R/R_F are obtained from the best-fit electron density (ED) profiles shown in Figures 1b and 2b using the optimal structural parameters via a slab model.[11,20] From left to right, the ED profiles feature three regions that can be readily associated with the subphase, single-particle-thick layer, and the vapor (or gas) phase (the vapor-suspension interface is set at z = 0).

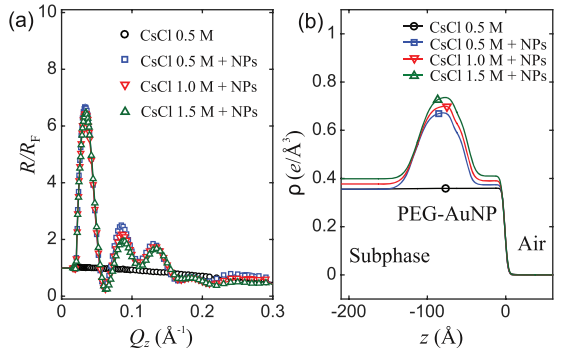

Figure 1. (a) R/R_F data for CsCl solutions at concentrations of 0.5−1.5 M in the presence of the same amount of PEG-AuNPs in suspensions. The solid lines are best-fit using the optimal structural parameters through data refinement. (b) Corresponding ED profiles that yield the best-fit to the R/R_F data.

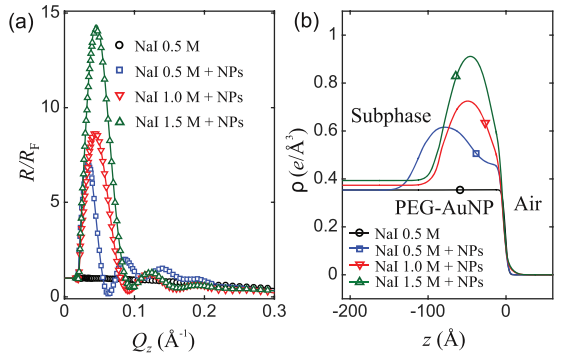

Figure 2. (a) R/R_F data for NaI solutions at concentrations of 0.5−1.5 M in the presence of the same amount of PEG-AuNPs in suspensions. The solid lines are best-fit using the optimal structural parameters through data refinement. (b) Corresponding ED profiles that yield the best-fit to the R/R_F data.

The ED profiles of the assembled films of PEG-AuNPs on the CsCl solutions at different salt concentrations, in Figure 1, show that the uniform film is at the suspension/vapor interface and that the film does not change significantly as the salt concentration varies from 0.5 to 1.5 M. The length-scale of the ED-enhanced region on the ED profile (approximately 10−15 nm) is evidence that a monolayer of a single-particle depth is formed at the aqueous surface.[1,4,14] An interesting feature of the ED profiles of PEG-AuNPs with CsCl is a flat region of approximately ∼5 nm thick between the vapor phase and the enhanced ED peak. We attribute this flat region to compressed PEG chains dangling outward directly in contact with the gas phase, as has been observed and proposed previously[1,14] for crystalline PEG-AuNPs films that are induced by various salts, e.g., K_2CO_3, NaCl, KCl, $MgCl_2$, K_2SO_4, Cs_2SO_4, and K_3PO_4.[4,5,14] By contrast, the ED profiles from PEG-AuNPs with NaI in the suspensions change significantly both in shape and magnitude as the concentration increases from 0.5 to 1.5 M. The increase in the area under the peaked region of the ED is evidence for increased enrichment of PEG-AuNPs at the surface. For 0.5 M NaI, the ED profile is somewhat similar to that obtained with CsCl, albeit with broader interfaces. This is a signature of enhanced surface roughness in the film, likely due to random staggering AuNPs with respect to the surface.

DOI: 10.1021/acs.langmuir.9b02966
Langmuir 2020, 36, 311−317

Table 1. Summary of XRR and GISAXS Analysis[a,b,c,d]

salt	reflectivity			GISAXS			
	Γ_e (±10%) [e/Å^2]	A_{XRR} (±10%) [nm^2]	A_{XRR} (±10%) [$\pi D^2/4$]	Q_1 (±2%) [Å^{-1}]	a (±2%) [nm]	A_{GISAXS} (±2%) [nm^2]	A_{GISAXS} (±2%) [$\pi D^2/4$]
CsCl 0.5 M	19.9	774	12.7	0.0250	29.0	728	12.0
CsCl 1.0 M	19.9	770	12.7	0.0250	29.0	728	12.0
CsCl 1.5 M	20.6	740	12.2	0.0250	29.0	728	12.0
NaI 0.5 M	22.1	697	11.5	0.026	27.9	674	11.1
NaI 1.0 M	21.8	701	11.5	0.028	25.9	581	9.6
NaI 1.5 M	31.8	480	7.9	n/a	n/a	n/a	n/a

[a]The surface excess Γ_e is determined with eq 1. [b]A_{XRR} is the average area of PEG-AuNP in the film estimated from the XRR (provided in nm^2 units and also in units of the largest cross-sectional area, i.e., $\pi D^2/4$, for a AuNP). [c]Q_1 is the fundamental Bragg peak of the assumed hexagonal symmetry that gives the hexagonal lattice constant a and A_{GISAXS} is the corresponding area per particle calculated using a. [d]The upper bound in the relative uncertainties is in the parenthesis.

As the concentration of NaI increases, the ED profile becomes more structured, and more importantly, the main peak sharpens significantly indicating more tightly bound AuNPs at the surface due to the effect of iodine on the confirmation of PEG.[21,22]

In fact, with reasonable assumptions, using the space-filling model,[11] we can readily determine the average area per AuNP at the surface (denoted as A_{XRR}) from the ED profiles. We first calculate the surface electron excess Γ_e as follows

$$\Gamma_e = \int_{-\infty}^{0} [\rho(z) - \rho_{sol}]dz \quad (1)$$

where $\rho(z)$ and ρ_{sol} are the ED obtained from the XRR (Figures 2 and 1) and the bulk solution, respectively. For example, for 1.5 M CsCl and NaI solutions, ρ_{CsCl} = 0.40 e/Å^3 and ρ_{NaI} = 0.39 e/Å^3, respectively. For dry PEG, we calculate ρ_{PEG} = 0.37 e/Å^3, which is very close to that of the solution, thus it is virtually eliminated from the surface excess. The surface excess Γ_e is to a good approximation mainly due to the core AuNPs and can be independently calculated as follows

$$\Gamma_e = \frac{V_{AuNP}(\rho_{Au} - \rho_{sol})}{A_{XRR}} \quad (2)$$

where $V_{AuNP} = \pi D^3/6$ is the volume of a AuNP of diameter D and ρ_{Au} = 4.67 e/Å^3 is the ED of bulk Au. Using eqs 1, 2 and D = 8.8 nm (obtained by small-angle X-ray scattering),[1,2] we determine A_{XRR}, as listed in Table 1.

Grazing Incidence Small-Angle X-ray Scattering (GISAXS). Figure 3a shows 2D images of (Q_{xy}, Q_z) intensity maps obtained by GISAXS from surfaces of PEG-AuNP aqueous suspensions mixed with 1 M NaCl, CsCl, and NaI, as indicated. The scattering rods along Q_z are typical Bragg reflections from 2D ordered systems. Line-cuts obtained by integration over Q_z = 0.02−0.1 Å^{-1} profile shown in Figure 3b feature sharp peaks for CsCl subphases, with a prominent fundamental peak at $Q_{xy} = Q_1$ = 0.025 Å^{-1} and higher-order peaks at positions that are allowed for the 2D hexagonal lattice (i.e., $Q_{xy}/Q_1 = \sqrt{3}, \sqrt{4}, \ldots$ up to $\sqrt{13}$). The corresponding interparticle distance among the PEG-AuNP on the CsCl subphase is approximately 29 nm, which is much smaller than the hydrodynamic radius (D_h) of the PEG-AuNPs (35−40 nm grafted with PEG; molecular weight 6000 Da).[1] This suggests that the PEG corona surrounding the AuNPs shrinks as the PEG-AuNPs migrate to the interface, with sufficient flexibility to pack into the hexagonal structure. This is consistent with the current picture on the phase-separation behavior of PEG in salt solutions, where salt is expelled from the polymer region leading to enhanced polymer−polymer interactions that in our case lead to the shrinking of the corona.[22,23] By contrast, the intensity versus Q_{xy} profiles for the NaI subphase, under otherwise identical conditions as those for the CsCl subphase, feature much broader peaks hindering unambiguous crystallographic indexing. Nevertheless, the broadened peaks are indicative of short-range order (SRO) among surface-bound PEG-AuNPs, likely with a hexagonal motif. Based on the GISAXS data, we extract the lattice constant and the average area per AuNP (denoted as A_{GISAXS}) for the different solutions, as listed in Table 1. Despite the inferior surface crystallization in the presence of NaI, the identification of Q_1 shows the significantly larger surface density of PEG-AuNPs than that with CsCl for the same concentrations. The systematic larger

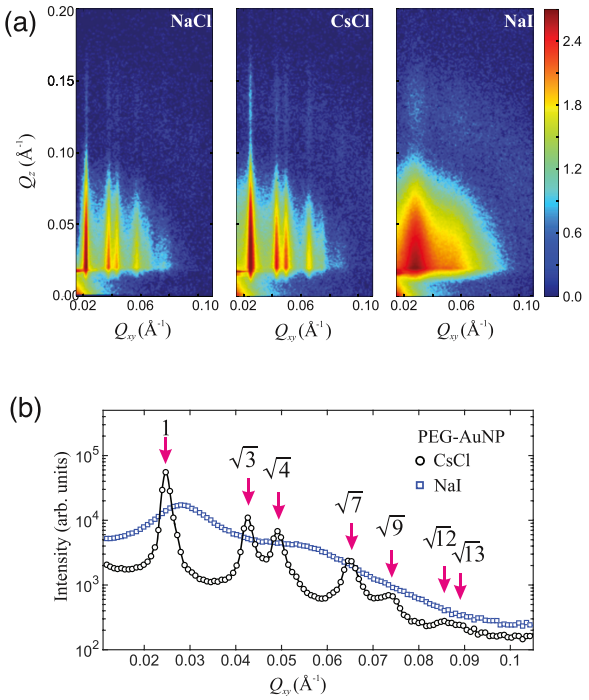

Figure 3. GISAXS data for CsCl and NaI solutions at a comparable concentration and in the presence of PEG-AuNPs. (a) GISAXS intensities as a function of Q_z and Q_{xy}, organized as colormaps. $Q_z = 2\pi(\sin\alpha_i + \sin\alpha_f)/\lambda$. The left panel to the right panel, the subphase contains 1 M of NaCl, CsCl, and NaI. (b) GISAXS intensity integrated over Q_z = 0.02−0.1 Å^{-1} for PEG-AuNP suspensions in the presence of CsCl or NaI, each of which is a concentration of 1.0 M.

DOI: 10.1021/acs.langmuir.9b02966
Langmuir 2020, 36, 311−317

A_{XRR} extracted from the XRR compared to A_{GISAXS} determined from GISAXS is expected, as the XRR averages over crystalline and void regions.

The trend of GISAXS profiles varying with salt concentrations is different for CsCl and NaI subphases, shown in Figure 4. The line-cut profiles along the horizontal direction

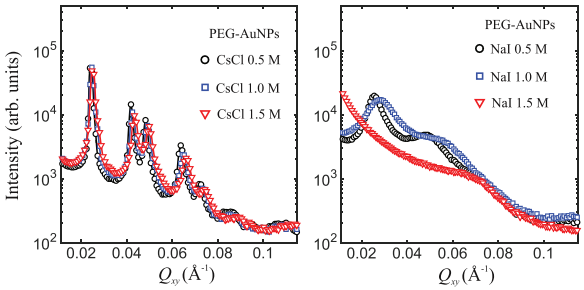

Figure 4. GISAXS intensity line-cut integrated over Q_z = [0.02−0.1] Å^{-1} for incremental bulk concentration levels. Left panel: CsCl subphases; right panel: NaI subphases.

remain almost unvaried with the CsCl concentration, which is quite consistent with the XRR results for a saturated surface. On the contrary, they vary quite significantly with the NaI concentration. Although the interference peaks are diffuse, they shift to higher Q_{xy} and become less defined with the NaI concentration. More importantly, the GISAXS lacks interference features at the highest NaI concentration (i.e., 1.5 M) tested within the accessible Q_{xy} range. The lack of the well-defined Bragg reflections suggests that the surface-bound PEG-AuNPs are arranged in almost an amorphous state.

Structural Model of Nanoparticle 2D-Assembly on Surfaces. Based on the surface X-ray scattering data analysis above, it is evident that the salt species in the bulk influence the surface density and arrangement of PEG-AuNPs at the aqueous surface.[4] Since NaCl and CsCl both promote practically indistinguishable 2D crystallization for the same bulk salt concentrations, one can conclude that the Cs^+ and Na^+ cations bear a similar role in the 2D crystallization. We note that a similar conclusion on these two salts has been reached while examining their effect on the biphase separation of PEG in their solutions.[22] By contrast, NaI is less capable of promoting surface superlattice formation compared to NaCl or CsCl, indicating that the anion I^- behaves differently than Cl^-, in two aspects. First, although the surface density of AuNPs reaches saturation at about 0.5 M of CsCl, it continues to increase with NaI concentration, as evidenced by XRR and GIXSAS. Second, the XRR clearly shows that the effective thickness of the film formed at the interface gets thinner with the addition of NaI. Both observations suggest that the PEG corona is affected more strongly in the presence of I^- by shrinking the PEG corona, facilitating a higher population of PEG-AuNPs at the interface. We propose that both salts shrink the corona, however, CsCl keeps the corona in spherical and/or flexible conformations that promote a high-quality hexagonal ordering, while NaI shrinks the corona even more into a rigid and collapsed state that upon populating the surface yields poorer crystallinity. Indeed, the GISAXS measurements of NaI solutions exhibit much broader Bragg reflections for surface PEG-AuNPs that at the highest tested bulk NaI concentration indicate an amorphous packing. Meanwhile, the corresponding XRR results show a more confined, monoparticle layer with an increased maximum in the ED profile.

Figure 5 depicts the conformation and in-plane ordering of PEG-AuNPs in the presence of CsCl (or NaCl) and NaI. For

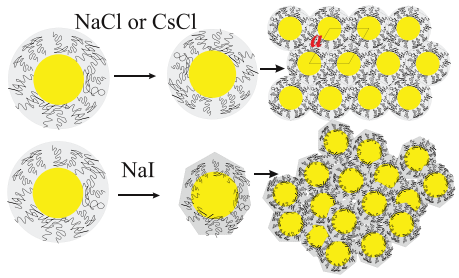

Figure 5. (Top) Illustration of PEG-AuNPs in a NaCl or CsCl solution where the hydrodynamic radius is affected only marginally. NaCl or CsCl induces migration of the PEG-AuNPs to the vapor/liquid interface where the PEG-AuNPs arrange in a highly ordered two-dimensional hexagonal structure with the nearest neighbor (NN) distance that is significantly smaller than the hydrodynamic diameter. (Bottom) In the presence of NaI, the PEG-AuNPs are more efficiently driven to the vapor/liquid interface (higher surface density), however the in-plane ordering is only short range and the average NN distances are much smaller than those achieved with NaCl or CsCl. This suggests that the PEG corona is tucked in closer to the surface of the AuNP, is less spherical, and is not sufficiently flexible to pack in a hexagonal structure.

suspensions where NaCl or CsCl induces migration of the PEG-AuNPs to the vapor/liquid interface, the particles arrange in a highly ordered two-dimensional hexagonal structure with a nearest neighbor (NN) distance that is significantly smaller than the hydrodynamic diameter. Increasing CsCl concentration above 0.5 M does not lead to increased surface density and barely affects the hexagonal lattice constant. In the presence of NaI, the PEG-AuNPs are more efficiently driven to the vapor/liquid interface (i.e., higher surface density), however the in-plane ordering is only short-range-ordered and the average NN distances are much smaller than those achieved with NaCl or CsCl. This suggests that the PEG corona is tucked in closer to the surface of the AuNP, less spherical, and not sufficiently flexible to pack into a hexagonal structure. Equivalently, from the perspective of molecular interactions, long and flexible grafted PEG chains provide certain steric (entropic) repulsion that facilitate hexagonal packing.[1] By contrast, the van der Waals attraction may dominate among the AuNPs enwrapped with collapsed and thus rigid PEG chains and make the particles sticky, resulting in irregular packing. To further confirm the unusual effect of iodide ions on the PEG corona we discuss below DLS measurements of PEG-AuNPs in suspensions with the aforementioned salts.

Dynamic Light Scattering. The interaction among the PEG-AuNPs is mediated by the PEG corona, which governs the assembly process on the aqueous surface. DLS studies have shown that the D_h of PEG-AuNPs changes only mildly with the addition of salts.[1] Figure 6 shows the DLS intensity distributions against the D_h for AuNPs and PEG-AuNPs in aqueous solutions at various salt concentrations. The D_h at the highest DLS intensity percentage is referred to as $\langle D_h \rangle$. Figure 6a shows that the $\langle D_h \rangle$ increases from ∼12.2 nm for bare AuNPs to ∼36.6 nm for AuNPs grafted with the PEG corona.

DOI: 10.1021/acs.langmuir.9b02966
Langmuir 2020, 36, 311−317

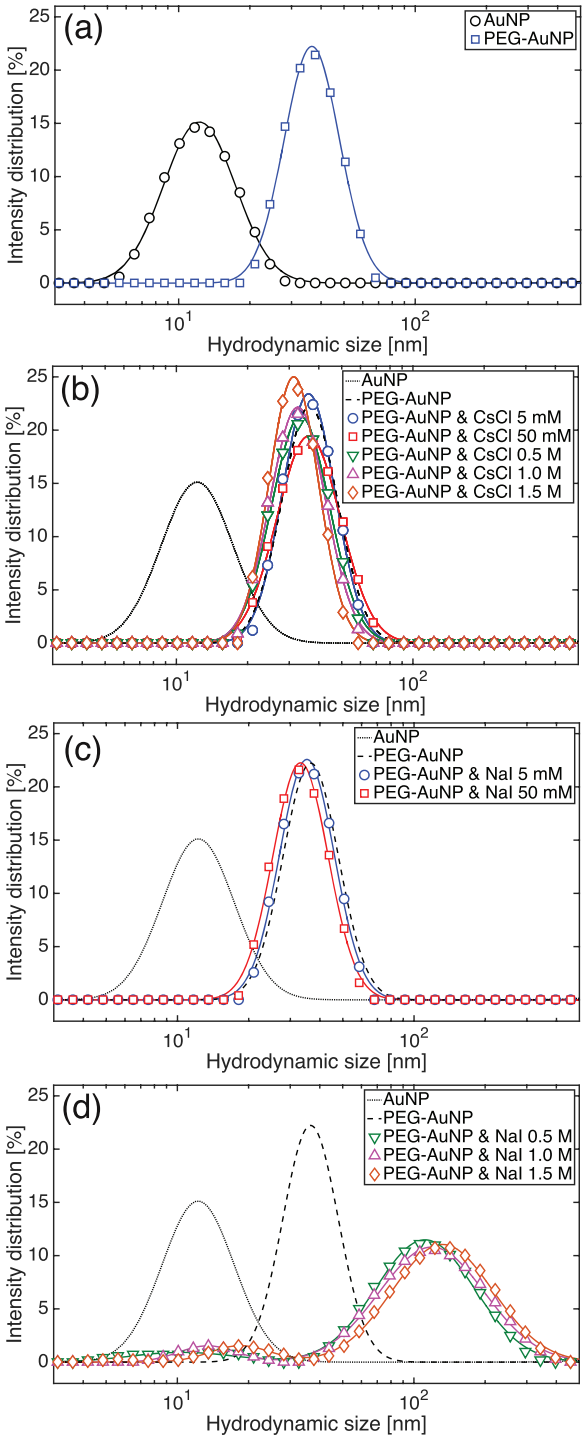

Figure 6. DLS intensity distributions of PEG-AuNPs in the presence and absence of salts. DLS data for AuNPs (coated with only citrate ligands) and PEG-AuNPs suspensions (shown in (a)) are provided for comparison (dotted and dashed lines in (b)−(d)). (a) DLS data for AuNP (bare surface) and PEG-AuNP suspensions in the absence of salts. (b) DLS data for PEG-AuNP suspensions in the presence of CsCl at concentrations of 5 mM−1.5 M. (c) DLS data for PEG-AuNP suspensions in the presence of NaI at concentrations of 5 and 50 mM. (d) DLS data for PEG-AuNP suspensions in the presence of NaI at concentrations of 0.5−1.5 M.

Based on these two values, the thickness of the PEG corona in the bulk is estimated at ∼12 nm.

Figure 6b shows that the presence of CsCl barely changes the D_h distribution of the PEG-AuNPs in suspensions consistent with previous results of NaCl and K_2CO_3 in the suspensions.[1] Indeed, the D_h distribution changes from 36.6 nm for a suspension with no salt to 31.3 nm for a suspension at 1.5 M CsCl. Although small, the shrinking tendency of the corona in the presence of salt is consistent with our XRR and GISAXS results above. This suggests that the PEG in the corona is in the θ-point state even at high salt concentrations. Figure 6c shows that the D_h distribution of PEG-AuNPs changes just slightly at NaI concentrations of 5−50 mM. However, a drastic change in the D_h distribution occurs for NaI concentration at 0.5 M and higher, as shown in Figure 6d. The majority of the size distribution shifts to high $\langle D_h \rangle$ ∼110 nm, which is about three times the $\langle D_h \rangle$ without salt, likely arising from the initiation of the assembly into small clusters of PEG-AuNPs in the bulk. There is also a small but detectable peak at low $\langle D_h \rangle$ ∼20 nm, which suggests that the corona shrinks significantly and no longer in the θ-state. Indeed, the number distribution (see the Supporting Information) suggests that the suspended particles of collapsed corona greatly outnumber the clusters. The PEG-AuNPs in the presence of relatively high concentrations of NaI thus either aggregate into small clusters or remain independent with a collapsed PEG corona. The quantitative dependence of $\langle D_h \rangle$ on the salt concentrations is summarized in Figure 7.

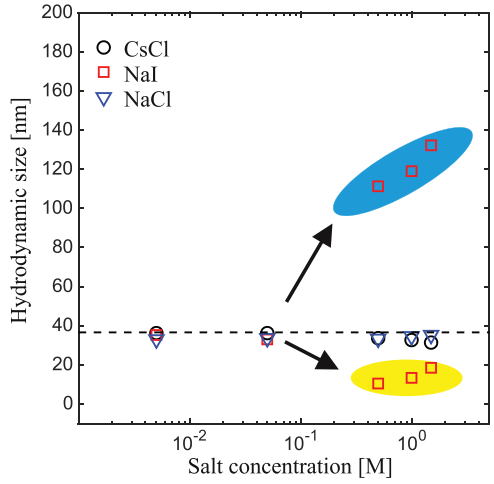

Figure 7. $\langle D_h \rangle$ of PEG-AuNPs in suspensions as a function of salt concentrations. The $\langle D_h \rangle$ of PEG-AuNPs barely changes in response to the presence of NaCl and CsCl. On the other hand, there seems a threshold concentration of NaI in between 50 and 500 mM, beyond which there is a significant increase in $\langle D_h \rangle$, most likely resulting from the clustering of PEG-AuNPs. Meanwhile, there is also a significant reduction in $\langle D_h \rangle$, likely resulting from the collapse of PEG coronas.

The equivalent number and volume distribution based on the DLS results are shown in the Supporting Information. Indeed, they all show that the majority of the PEG-capped AuNPs shrink mildly in the apparent hydrodynamic size in the presence of the salts. Above the some critical NaI concentration, most PEG-capped AuNPs appear as if their PEG corona is collapsed.

It was reported that halide ions have an affinity toward the AuNPs and replace the stabilizing citrate ions at different degrees, and iodine ions have the strongest affinity leading to aggregation and fusions of AuNPs.[24,25] In this study, we argue

DOI: 10.1021/acs.langmuir.9b02966
Langmuir 2020, 36, 311−317

that the adsorbed iodine, if any, cannot remove the surface-grafted PEG chains due to the strong gold−sulfur bonding, even though the nature of such bonding is still under investigation.[26,27] Otherwise, the iodine-capped AuNPs will aggregate and precipitate. Indeed, the bare surface AuNP solutions spontaneously turn from red-wine color to blue almost instantly once salts (e.g., NaCl or NaI) are mixed to a final concentration of 0.5 M and turn transparent after overnight sediment. Tiny, black precipitates are typically observed at the bottom of the solutions. Regarding the interaction among PEG chains and halide ions, earlier studies show that the I^- ions tend to associate with PEG in a PEG-rich phase much more than other halide ions (i.e., Cl^- and Br^-).[28] We surmise that the strong association among I^- and PEG in the PEG-rich phase, here the PEG corona, may remove more water molecules from the PEG and constrain the PEG flexibility significantly, leading to its collapse.

CONCLUSIONS

Using surface sensitive X-ray diffraction and dynamic light scattering, we examine aspects of the assembly at the vapor/suspension interface and the bulk conformation of PEG-AuNPs in the presence of CsCl and NaI in the suspension. Although CsCl is a representative of many electrolytes, we find that NaI behaves differently. We find ion-specific effect in these simple salts regarding the conformation of grafted PEG on AuNPs that impacts their assembly process at the vapor/solution interface. Using surface sensitive X-ray diffraction methods, previous studies have shown that the presence of practically any electrolyte, regardless of pH (pH in the range 2−11), in the suspension, drives the PEG-AuNPs to the aqueous surface to form a monoparticle layer, that for most salts leads to ordering of the PEG-AuNPs into high-quality 2D hexagonal crystal structures.[4,5] However, in the presence of I^- in the suspension, although a narrow monoparticle film is formed, the AuNPs' arrangement is only very short-range ordered or even amorphous, depending on the iodide concentration. In addition, I^- in the suspension induces significantly higher surface densities of the PEG-AuNPs than any of those achieved with other electrolytes (CsCl or NaCl, for instance).

We correlate the different assemblies at the interface with the conformation of the PEG corona in the presence of salts. Complementary DLS results of PEG-AuNPs in the presence of these salts are consistent with the assertion that PEG corona collapses in the presence of I^-. We argue that that the grafted PEG preserves its θ-point state in the presence of most electrolytes, a condition that facilitates long-range order at the interface. On the other hand, when the PEG corona collapses, the assembly is of higher density but the in-plane packing tends to be amorphous. We surmise that NaI turns the PEG-AuNPs into an effective hard nonspherical nanoparticle that can only pack in short-range order. We propose that for most salts, the effective repulsion among particles leads to hexagonal packing, while for NaI, the collapsed PEG corona tends to favor attraction (i.e., van der Waals) of multiple particles that cannot readily readjust to form an ordered array.

ASSOCIATED CONTENT

Supporting Information

The Supporting Information is available free of charge at https://pubs.acs.org/doi/10.1021/acs.langmuir.9b02966.

Dynamic light scattering (DLS) results (number distribution and volume distribution) for PEG-AuNPs; photographs showing the phase separation of PEG solutions in the presence of salts (PDF)

AUTHOR INFORMATION

Corresponding Authors

*E-mail: wenjiew@ameslab.gov (W.W.).
*E-mail: vaknin@ameslab.gov (D.V.).

ORCID

Wenjie Wang: 0000-0002-7079-1691
Surya Mallapragada: 0000-0002-9482-7273
David Vaknin: 0000-0002-0899-9248

Notes

The authors declare no competing financial interest.

ACKNOWLEDGMENTS

We thank Jack J. Lawrence for technical support in sample preparation. We thank Dr Honghu Zhang for discussion on the results. The research was supported by the U.S. Department of Energy, Office of Basic Energy Sciences, Division of Materials Sciences and Engineering. Ames Laboratory is operated for the U.S. Department of Energy by Iowa State University under Contract No. DE-AC02-07CH11358. NSF's ChemMatCARS Sector 15 is principally supported by the Divisions of Chemistry (CHE) and Materials Research (DMR), National Science Foundation, under grant number NSF/CHE-1834750. Use of the Advanced Photon Source, an Office of Science User Facility operated for the U.S. Department of Energy (DOE) Office of Science by Argonne National Laboratory, was supported by the U.S. DOE under Contract No. DE-AC02-06CH11357.

REFERENCES

(1) Zhang, H.; Wang, W.; Mallapragada, S.; Travesset, A.; Vaknin, D. Macroscopic and tunable nanoparticle superlattices. *Nanoscale* **2017**, *9*, 164−171.

(2) Zhang, H.; Wang, W.; Akinc, M.; Mallapragada, S.; Travesset, A.; Vaknin, D. Assembling and ordering polymer-grafted nanoparticles in three dimensions. *Nanoscale* **2017**, *9*, 8710−8715.

(3) Ha, J.-M.; Lim, S.-H.; Dey, J.; Lee, S.-J.; Lee, M.-J.; Kang, S.-H.; Jin, K. S.; Choi, S.-M. Micelle-Assisted Formation of Nanoparticle Superlattices and Thermally Reversible Symmetry Transitions. *Nano Lett.* **2019**, *19*, 2313−2321.

(4) Zhang, H.; Wang, W.; Mallapragada, S.; Travesset, A.; Vaknin, D. Ion-Specific Interfacial Crystallization of Polymer-Grafted Nanoparticles. *J. Phys. Chem. C* **2017**, *121*, 15424−15429.

(5) Nayak, S.; Fieg, M.; Wang, W.; Bu, W.; Mallapragada, S.; Vaknin, D. Effect of (Poly)electrolytes on the Interfacial Assembly of Poly(ethylene glycol)-Functionalized Gold Nanoparticles. *Langmuir* **2019**, *35*, 2251−2260.

(6) Kanehara, M.; Kodzuka, E.; Teranishi, T. Self-Assembly of Small Gold Nanoparticles through Interligand Interaction. *J. Am. Chem. Soc.* **2006**, *128*, 13084−13094.

(7) Si, K. J.; Chen, Y.; Shi, Q.; Cheng, W. Nanoparticle superlattices: The roles of soft ligands. *Adv. Sci.* **2018**, *5*, No. 1700179.

(8) Grzelczak, M.; Vermant, J.; Furst, E. M.; Liz-Marzan, L. M. Directed Self-Assembly of Nanoparticles. *ACS Nano* **2010**, *4*, 3591−3605.

(9) Srivastava, S.; Nykypanchuk, D.; Fukuto, M.; Gang, O. Tunable Nanoparticle Arrays at Charged Interfaces. *ACS Nano* **2014**, *8*, 9857−9866.

(10) Srivastava, S.; Nykypanchuk, D.; Fukuto, M.; Halverson, J. D.; Tkachenko, A. V.; Yager, K. G.; Gang, O. Two-Dimensional DNA-

DOI: 10.1021/acs.langmuir.9b02966
Langmuir 2020, 36, 311−317

Programmable Assembly of Nanoparticles at Liquid Interfaces. *J. Am. Chem. Soc.* **2014**, *136*, 8323−8332.
(11) Vaknin, D. X-ray Diffraction and Spectroscopy Techniques for Liquid Surfaces and Interfaces. In *Characterization of Materials*, 2nd ed.; Kaufmann, E. N., Ed.; John Wiley & Sons: New York, NY, 2012; Vol. 2, pp 1393−1432.
(12) Wang, W.; Zhang, H.; Kuzmenko, I.; Mallapragada, S.; Vaknin, D. Assembling bare Au nanoparticles at positively charged templates. *Sci. Rep.* **2016**, *6*, No. 26462.
(13) Zhang, H.; Wang, W.; Hagen, N.; Kuzmenko, I.; Akinc, M.; Travesset, A.; Mallapragada, D.; Vaknin, S. Self-assembly of DNA functionalized gold nanoparticles at the liquid-vapor interface. *Adv. Mater. Interfaces* **2016**, *3*, No. 1600180.
(14) Wang, W.; Zhang, H.; Mallapragada, S.; Travesset, A.; Vaknin, D. Ionic depletion at the crystalline Gibbs layer of PEG-capped gold nanoparticle brushes at aqueous surfaces. *Phys. Rev. Mater.* **2017**, *1*, No. 076002.
(15) Zhang, H.; Nayak, S.; Wang, W.; Mallapragada, S.; Vaknin, D. Interfacial Self-Assembly of Polyelectrolyte-Capped Gold Nanoparticles. *Langmuir* **2017**, *33*, 12227−12234.
(16) Vaknin, D.; Wang, W.; Islam, F.; Zhang, H. Polyethyleneglycol-mediated self-assembly of magnetic nanoparticles at the liquid/vapor interface. *Adv. Mater. Interfaces* **2018**, *5*, No. 1701149.
(17) Wu, C.; Wang, X. Globule-to-coil transition of a single homopolymer chain in solution. *Phys. Rev. Lett.* **1998**, *80*, 4092−4094.
(18) Goldsack, D. E.; Franchetto, R. Viscosity of concentrated electrolyte-solutions. 1. Concentration-dependence at fixed temperature. *Can. J. Chem.* **1977**, *55*, 1062.
(19) Jenkins, H. D. B.; Marcus, Y. Viscosity B-coefficient of ions in solution. *Chem. Rev.* **1995**, *95*, 2695−2724.
(20) Tolan, M. *X-Ray Scattering from Soft-Matter Thin Films: Materials Science and Basic Research*; Springer-Verlag, 1999.
(21) Lundberg, R. D.; Bailey, F. E.; Callard, R. W. Interactions of inorganic salts with poly(ethylene oxide). *J. Polym. Sci., Part A-1: Polym. Chem.* **1966**, *4*, 1563−1577.
(22) Bailey, F. E., Jr.; Callard, R. W. Some properties of poly(ethylene oxide) in aqueous solution. *J. Appl. Polym. Sci.* **1959**, *1*, 56−62.
(23) Florin, E.; Kjellander, R.; Eriksson, J. C. Salt effects on the cloud point of the poly(ethylene oxide)+ water system. *J. Chem. Soc., Faraday Trans. 1* **1984**, *80*, 2889−2910.
(24) Cheng, W.; Dong, S.; Wang, E. Iodine-Induced Gold-Nanoparticle Fusion/Fragmentation/Aggregation and Iodine-Linked Nanostructured Assemblies on a Glass Substrate. *Angew. Chem., Int. Ed.* **2003**, *42*, 449−452.
(25) Zhang, Z.; Li, H.; Zhang, F.; Wu, Y.; Guo, Z.; Zhou, L.; Li, J. Investigation of Halid-Induced Aggregation of Au Nanoparticles into Spongelike Gold. *Langmuir* **2014**, *30*, 2648−2659.
(26) Häkkinen, H. THe gold-sulfer interface at the nanoscale. *Nat. Chem.* **2012**, *4*, 443−455.
(27) Pensa, E.; Cortes, E.; Corthey, G.; Carro, P.; Vericat, C.; Fonticelli, M. H.; Benitez, G.; Rubert, A. A.; Salvarezza, R. The Chemistry of the Sulfur-Gold Interface: In Search of a Unified Model. *Acc. Chem. Rev.* **2012**, *45*, 1183−1192.
(28) Kumai, A.; Minagawa, Y. Photographic Properties of Polyethylene Oxide I. Interaction of Halide Ions with PEO. *J. Photogr. Sci.* **1970**, *18*, 91−93.

DOI: 10.1021/acs.langmuir.9b02966
Langmuir 2020, 36, 311−317